





Chlorite-Oxidized Oxyamylose (COAM) Has Antibacterial Activity and Positively Affects Skin Wound Healing

Rafaela Vaz Sousa Pereira ¹, Estefania Ugarte-Berzal¹, Jennifer Vandooren¹, Karin Nylander², Erik Martens¹, Lieve Van Mellaert ¹, Jo Van Damme¹, Jan Jeroen Vranckx³, Patrick Matthys¹, Tiina Alamäe⁴, Mia Phillipson², Triinu Visnapuu ⁴, Ghislain Opdenakker ¹

¹Department of Microbiology, Immunology and Transplantation, Rega Institute for Medical Research, KU Leuven, Leuven, Belgium; ²Department of Medical Cell Biology, Division of Integrative Physiology, Uppsala University, Uppsala, Sweden; ³Department of Development & Regeneration & Department of Plastic & Reconstructive Surgery, University Hospitals Leuven and KU Leuven, Leuven, Belgium; ⁴Department of Genetics, Institute of Molecular and Cell Biology, University of Tartu, Tartu, Estonia

Correspondence: Ghislain Opdenakker, Department of Microbiology, Immunology and Transplantation, Rega Institute for Medical Research, KU Leuven, Herestraat 49 Box 1044, Leuven, 3000, Belgium, Tel +32 16 37 9020, Fax +32 16 33 3026, Email ghislain.opdenakker@kuleuven.be

Purpose: To verify the antibacterial and immunomodulatory effects of the amylose derivative – chlorite-oxidized oxyamylose (COAM) – in a skin wound setting.

Methods: In vitro antibacterial effects of COAM against opportunistic bacterial pathogens common to skin wounds, including *Staphylococcus aureus* and methicillin-resistant *Staphylococcus aureus* (MRSA), were determined by cultivation methods. The effects of COAM on myeloid cell infiltration into full thickness skin wounds were investigated in wild-type and in transgenic CX₃CR1-GFP mice.

Results: On the basis of in vitro experiments, an antibacterial effect of COAM against *Staphylococcus* species including MRSA was confirmed. The minimum inhibitory concentration of COAM was determined as 2000 µg/mL against these bacterial strains. Control full thickness skin wounds yielded maximal neutrophil influxes and no additive effect on neutrophil influx was observed following topical COAM-treatment. However, COAM administration increased local CX₃CR1 macrophage counts at days 3 and 4 and induced a trend towards better wound healing.

Conclusion: Aside from its known broad antiviral impact, COAM possesses in vitro antibacterial effects specifically against Gram-positive opportunistic pathogens of the skin and modulates in vivo macrophage contents in mouse skin wounds.

Keywords: antimicrobial, wound healing, neutrophils, macrophages, amylose derivative, *Staphylococcus*

Introduction

New developments in regenerative medicine with the use of mobilized or in vitro-modified stem cells have generated new avenues and opportunities for the treatment of many debilitating diseases, including chronic skin wounds.¹ However, efforts towards cell-based therapies and their application in hospitals are costly and time-consuming. Furthermore, because of Major Histocompatibility Complex (MHC) restrictions by the host immune system, therapies with cells from human donors are restricted to auto-transplantation of, eg, stem cells from wounded patients. Human cell therapy with universally applicable donor tissue does not yet exist.^{2,3}

A common medical problem is impaired healing of skin wounds, resulting in chronic, nonhealing wounds. For example, aging populations are increasing in numbers, resulting in increased numbers of patients with pressure (or decubitus) sores. In Europe and the US, elderly with decubitus wounds represent cohorts of millions of often hospitalized patients. The estimated prize of pressure sore treatment amounts to an annual recurrent cost of more than 10 billion dollars in the US alone.⁴

Aside pressure ulcers, common in immobilized elderly, diabetic foot ulcers, burns, traumata, impaired healing after radiotherapy, vascular insults (eg, venous thrombosis) and infections create necrotic wounds in urgent need of better treatments. As an alternative to the time-consuming and costly cell therapies, the application of various growth factors, including platelet-derived growth factor (PDGF), vascular endothelial growth factor (VEGF) and other cytokines have been probed with limited success. A possible explanation is the insight that the natural healing process of acute wounds is fine-tuned in time and space. In addition, with single host cell types or molecules it is impossible to mimic the synchronized healing process, involving multiple cell types, or to force it towards physiological healing with its sequential appearance and disappearance of specific leukocyte types.⁵ Solutions to advance our knowledge are (i) definition of locoregional and temporal cellular changes and molecular expression levels, and (ii) testing and modifying various pharmacological agents to efficiently aid wound healing.^{1,5} Histologically, sterile acute skin wounds, for instance after skin abrasion or excision for skin transplantation purposes, develop a rich dermal granulation reaction. In addition, such wounds are wet, rather than dry and, at the edges, keratinocytes grow as to fill the epithelial layers. Some of these processes in acute wounds are comparable to those of severe inflammatory reactions or skin infections.

Intact skin is a perfect antimicrobial barrier against bacteria and viruses and is, at the external side, inhabited by the so-called skin microbiome. When the skin as an integument is broken and the wound is not properly disinfected and treated, infection is imminent, in particular with common papillomaviruses causing warts and with bacterial species including *Staphylococcus aureus* strains. Skin infections need to be avoided, as these impair the healing process and contribute to the development of chronic wounds.⁶ The most frequently encountered bacteria in skin infections are *Staphylococcus aureus* strains including the methicillin resistant variant — MRSA.⁷ Other bacteria mostly related to skin infections are *Pseudomonas aeruginosa*, *Escherichia coli*, *Acinetobacter* spp., and coagulase-negative staphylococci such as *Staphylococcus epidermidis*.⁷ Antibiotic resistance is a crucial problem in the management and treatment of infected wounds.⁸ Therefore, the interest in the search and development for alternative antimicrobial agents, including capped nanocomposites and platelet-rich plasma, acting also on resistant bacterial strains has recently been significantly increased.^{9–11} Antimicrobial properties of several polysaccharides from bacteria and fungi have been studied. Two major targets of their action that have been pointed out in recent literature are biofilm formation and membrane integrity of microbes.^{12–14} As discussed later for comparison, polymers, hydrogels and other scaffolds may possess intrinsic antibacterial activities.^{15,16}

We have previously studied the antiviral mechanism of action of a chemically modified polysaccharide-derivative, chlorite-oxidized oxyamylose (COAM) against lethal mengovirus in mice. This antiviral agent was demonstrated to recruit myeloid cells through binding of granulocyte chemotactic protein-2 (GCP-2/CXCL6).¹⁷ Next, we demonstrated that COAM acted as a mimetic of glycosaminoglycan (GAG) and exposed chemokines more efficiently, due to its higher affinities towards the chemokines than those of GAGs. Remarkably, the exposed chemokines remained functionally active and, thereby, COAM may direct cells to specific body compartments.¹⁸ Within the context of skin inflammation, leukocyte recruitment by COAM has already been studied in the mouse air pouch model.¹⁹ After 24 h, COAM dose-dependently induced maximal local neutrophilia (60% of infiltrated leukocytes) and a relative decrease in mononuclear cell numbers, both macrophages and lymphocytes. It needs to be stressed that these observations represent measurements of pharmacological inflammatory effects of COAM in normal skin with intact epidermal and dermal layers.¹⁹

Here, we investigated the role of the polysaccharide-derivative COAM as a novel antimicrobial agent against skin-related bacteria and as immunomodulatory compound in skin wound healing. As target bacteria, we mostly addressed *Staphylococcus* species, as they are commonly present in infected wounds. Inflammatory effects of COAM on mice with induced skin wounds as a comparison of the above-mentioned inflammation in skin with an intact epithelial barrier were investigated.

Materials and Methods

Bacterial Strains and Media

Bacterial strains *Staphylococcus aureus* subsp. *aureus* (ATCC 6538), *Staphylococcus aureus* subsp. *aureus* (ATCC 6538P), methicillin-resistant *Staphylococcus aureus* subsp. *aureus* (MRSA, UZ Gasthuisberg collection, Belgium),

Staphylococcus epidermidis (ATCC 12228), biofilm-forming *Staphylococcus epidermidis* (ATCC 35984), *Pseudomonas aeruginosa* PAO1 (ATCC 15692), *Pseudomonas aeruginosa* PAO1 (ATCC BAA-47), *Bacillus subtilis* (EEUT VIL; CELMS microbe collection, Estonia), *Bacillus cereus* (ATCC 11778), *Escherichia coli* (EEUT EY; CELMS microbe collection, Estonia), were maintained on agar plates of Luria-Bertani (LB) medium, and grown at 30°C or 37°C on LB or Mueller-Hinton (MH) broth. LB broth contained (g/L): 10 g tryptone, 5 g yeast extract, 5 g NaCl. MH broth contained (g/L): 2 g beef extract, 1.5 g starch, 17.5 g casein hydrolysate. For agar plates preparation, 1.5% agar was added to the medium.

COAM Synthesis

COAM was prepared by two-step oxidation of amylose, as previously described.²⁰ Briefly, oxidation by sodium periodate cleaved the cyclic monosaccharide structures between two carbon atoms, yielding a polymer containing aldehyde functions called oxyamylose. In a second step of oxidation by sodium chlorite, the aldehyde functions are converted into carboxyl functions. The final product is referred to as chlorite-oxidized oxyamylose or COAM. COAM batches prepared were free of endotoxin and of protein contaminants, determined by Limulus amoebocyte lysate test and SDS-PAGE electrophoresis followed by Coomassie Brilliant Blue or silver staining, respectively.²¹ Cytotoxicity of COAM on cell cultures was previously studied, and, related to antiviral activity, COAM has a safety index (toxic versus active concentration) in excess of 10.²¹

Antimicrobial Tests

For bacteria growth curve determination, cultures grown overnight in MH medium were diluted to a final OD₆₀₀ 0.01 in Corning polystyrene clear flat-bottom 96-well microplates. The final volume per well was 0.1 mL. COAM was previously dissolved in Milli-Q water under sterile conditions to prepare a stock solution that was further diluted in the media to reach the final concentration of 1000 µg/mL per well. As a positive control, the bacterial strains were grown under the same conditions but without COAM. Tetracycline was used as antibiotic control at a final concentration of 50 µg/mL. Microplates were shaken at 30°C for 24 h and OD₆₀₀ was recorded using InfiniteM200 PRO microplate reader (Tecan Group Ltd.) equipped with Tecan i-control 1.7 software.

For minimum inhibitory concentration (MIC) assay, mid-log phase cultures at final OD₆₀₀ 0.01 were incubated with different concentrations of COAM in MH or LB medium. Corning polystyrene clear flat-bottom 96-well microplates were used and the final volume per well was 0.1 mL. Two-fold serial dilutions of COAM with final concentrations ranging between 15.6 µg/mL and 4000 µg/mL were used. The microplate was incubated for 20 h at 37°C and bacterial growth was determined by OD₆₀₀ measurement. MIC was defined as the lowest concentration of COAM resulting in no detectable bacterial growth in the above-mentioned conditions.

To determine the minimum bactericidal concentration (MBC), colony-forming units (CFU/mL) were determined in bacterial suspensions from MIC analysis (after 20 h incubation with or without COAM) and in the initial inoculum. Briefly, 80 µL of bacterial suspensions treated with COAM (2000 µg/mL, 4000 µg/mL and 8000 µg/mL) which showed no visible sign of growth were sub-cultured by the spread plate technique on sterile MH agar plates. For CFU determination of the initial inoculum and of control samples (without COAM), 10-fold dilutions (range of 1×10^{-3} – 1×10^{-6} dilutions) were plated to allow the counting of colonies. The plates were incubated at 37°C for 24 h, colonies were counted in the optimal dilution, and CFU/mL were calculated by the formula: CFU/mL = (number of colonies x dilution factor)/volume plated. For viability calculations, CFU/mL of the initial inoculum was taken as 100%. MBC was defined as the lowest concentration of COAM able to reduce 99.9% of bacterial viability compared with initial inoculum.

Wound Induction Models and Treatments

All procedures on mice conducted at KU Leuven were in accordance with the regulations of the European Union, Belgian and Flemish legislation, and approved by the local Ethics Committee (License number P270/2015, P128/2019, Belgium). Procedures performed at Uppsala University were approved by the Uppsala Regional Laboratory Animal Ethical Committee. Procedures with the use of bacteria strains were performed in agreement with the Belgian legislation

on biosafety and supervised by the KU Leuven Health and safety department (VGM). Excisional wounds of the full thickness of the skin were induced in the back of C57BL/6J (Jackson Laboratory) mice to evaluate the effect of COAM on the wound and its healing.²² Briefly, mice were anesthetized with ketamine (100 mg/kg) and xylazine (10 mg/kg) and all hair was removed from skin areas with the use of a shaver and hair removal cream. The skin was lifted in the mid-dorsal line, folded and punched through with a 4 mm disposable sterile biopsy punch (Robbins Instruments), creating one wound on each side of the dorsal midline. The procedure was repeated two more times, generating 6 wounds per animal at locations that were inaccessible by the individual animals. After wound induction, single mice were housed in individual cages, to avoid confounding animal interactions, including biting and licking of wounds by other animals.

For the experiments of wound infection, *S. aureus* and MRSA infections were induced immediately after injury and investigated.²³ The experiment consisted of two groups of animals for each bacterial strain: a negative control group and a COAM-treatment group. Control animals received vehicle (saline) together with bacteria inoculum (1×10^4 CFU) in a final volume of 10 μ L per wound. COAM-treated animals received COAM (1000 μ g diluted in saline) together with bacteria inoculum (1×10^4 CFU) in a final volume of 10 μ L per wound. Additionally, there were two control groups of non-infected animals: one receiving only saline and the other group receiving COAM treatment.

For the experiments aiming to investigate the effect of COAM on neutrophils, the wounds were topically treated with COAM immediately after injury. COAM was diluted in saline under sterile conditions and applied locally in a volume of 10 μ L per wound at the indicated doses (200 μ g, 1000 μ g and 2000 μ g), while the animal was still anesthetized and kept under an infrared heating lamp. The control group of mice received the same volumes of saline.

For the study of monocytes/macrophages infiltration, a wound was induced using a sterile punch needle (5 mm in diameter) on the left hindlimbs of isoflurane-anesthetized CX₃CR1-GFP mice (on C57BL/6J background, Jackson Laboratories).²⁴ Treatment with COAM (100 μ L with a concentration of 2 mg/mL, 200 μ g dose) was injected intradermally at four different locations in the dermis around the wound edge. Control mice received saline (vehicle) injected intradermally.

Bacterial Colonization Assessment in Infected Wounds

Following humane euthanasia, wounds were harvested 48 h after the infection/treatment and homogenized into 0.5 mL phosphate-buffered saline (PBS). 10-fold dilutions of wound homogenates were prepared (range of 1×10^{-1} to 1×10^{-6} dilutions) and plated on agar plates by the drop method, in which 20 μ L of each dilution were plated in triplicates. The plates were air dried and incubated at 37°C for 24 h. The colonies were counted in the optimal dilution, averaged and CFU count per wound was determined.

Flow Cytometry of Wound Cells

Following humane euthanasia, wounds were harvested using 6 mm punch biopsy to collect 2 mm wound margins for analysis. Three pools of 2 wounds per animal were chopped and digested with Liberase TL enzyme cocktail [0.35 mg/mL Liberase TL (Roche), 3 mg/mL Collagenase D (Roche) and 0.1 mg/mL DNase I (Roche)] for 2 h at 37°C.²⁵ After incubation, the samples were filtered through a 70- μ m strainer to remove undigested debris and to yield single-cell suspensions. Approximately 1×10^6 cells were incubated with the Fc-receptor-blocking antibodies anti-CD16/anti-CD32 (BD Biosciences) and with a Zombie Aqua™ viability dye (BioLegend) for 15 min. After washing with FACS buffer (0.5% bovine serum albumin (BSA); 2 mM EDTA in PBS), surface receptors were stained with BUV395-conjugated anti-CD45 (BD), BV786-conjugated anti-CD11b (BD), phycoerythrin (PE)-conjugated anti-Ly6G (eBioscience) and PE/Cy5-conjugated anti-F4/80 (eBioscience) for 30 min. Next, cells were washed and fixed with 0.37% formaldehyde in PBS. Cells were analyzed on a BD LSR Fortessa X20 with DIVA software. Results were further analyzed with the FlowJo software (BD Biosciences).

Monocyte/Macrophage Infiltration to the Wound and Wound Size Assessment

The recruitment of monocytes/macrophages to the wound was investigated using a noninvasive bioimaging technique at Uppsala University (IVIS spectrum, Living Image, PerkinElmer). In the CX₃CR1-GFP mice, all CX₃CR1⁺ cells (predominantly monocytes and macrophages) express Green Fluorescent Protein (GFP), which emission can be detected

by the IVIS camera, allowing imaging of CX₃CR1⁺ cell-infiltration during the process of wound healing. The infiltration of CX₃CR1⁺ cells was measured as the total limb radiance, that is, the number of photons per second per area (p/s/cm²/sr). Both hindlimbs were imaged and the radiance of the non-wounded hindlimb (right-hind limbs) in each mouse was subtracted from the radiance of the wounded hindlimb (left-hind limbs), thus excluding eventual background fluorescence.

Digital images of the wounds were captured, and a scale was included in the image allowing for quantification of wound size using the software ImageJ. Wound size is expressed as wound area per day and percent healed in relation to wound diameter on day 0, respectively.

Statistical Analysis

Data were presented as mean ± SEM. The data analysis was performed with GraphPad Prism Software (version 9.3.1), and differences were considered significant at P < 0.05. First, normality tests were applied and therefore the one-way ANOVA test was used when more than two groups were analyzed, otherwise the Student's two-tailed unpaired *t*-test was used. For data which did not follow normal distribution, non-parametric Kruskal–Wallis tests were applied. Kaplan–Meier estimator was used only to visually demonstrate the time point of wound closure.

Results

COAM Has Antibacterial Effects on *Staphylococcus* Species in vitro

COAM, a derivative of amylose, has been developed as a biodegradable antiviral agent.²⁰ Whereas originally believed to rely on induction of interferon, the antiviral mechanism of action of COAM was shown to rely on other mediators from neutrophils and macrophages.¹⁷ Considering that (i) a variety of polysaccharides and their derivatives possess antimicrobial effects^{12–14} and (ii) COAM modulates myeloid cells which also have antibacterial actions,²⁶ it is relevant to study whether COAM acts directly or indirectly on potentially pathogenic bacteria and exhibits antimicrobial effects.

First, the effect of 1000 µg/mL COAM as a potential antimicrobial compound was tested in vitro for various strains and species of opportunistic pathogens potentially abundant in the skin setting, including *S. aureus* (ATCC 6538), *S. epidermidis* (ATCC 12228), *B. subtilis* (EEUT VIL), *B. cereus* (ATCC 11778), *P. aeruginosa* PAO1 (ATCC 15692) and *E. coli* (EEUT EY) ([Supplementary Figure 1A–F](#)). The growth curves with and without the presence of COAM were recorded in MH medium and a strong inhibiting effect of COAM on staphylococci was discovered ([Supplementary Figure 1A](#) and [B](#)). A considerable effect of COAM was recorded on the growth of *B. subtilis* and *B. cereus*, with a clearly visible aggregation effect on cells, seen even by the naked eye ([Supplementary Figure 1C, D](#) and [G](#)). Small clumps of cells and aggregates were also visible under the microscope in the cultures of staphylococci (data not shown). The effect of 1000 µg/mL COAM was negligible towards Gram-negative bacteria *E. coli* and *P. aeruginosa* ([Supplementary Figure 1E](#) and [F](#)).

To further investigate the antibacterial effect of COAM, we performed minimum inhibitory concentration (MIC) assays for *S. aureus* ATCC 6538P and MRSA (UZ Gasthuisberg collection) strains in MH medium. Mid-log growth-phase bacteria were incubated for 20 h in MH medium with increasing concentrations of COAM (15.6 to 4000 µg/mL). The bacterial growth inhibition of *S. aureus* ATCC 6538P and MRSA was visible as the absence of culture turbidity when bacteria were incubated in the presence of 1000 µg/mL COAM or higher concentrations (data not shown). OD₆₀₀ measurements confirmed that COAM completely abolished bacterial growth at 2000 µg/mL, and we determined the MIC of COAM as 2000 µg/mL for the *S. aureus* strains ([Figure 1A](#) and [B](#)). MIC assays for *S. aureus* variants were also performed in LB medium and additional bacterial species were analyzed: *S. epidermidis* (ATCC 12228), biofilm-forming *S. epidermidis* (ATCC 35984) and *P. aeruginosa* (ATCC BAA-47) ([Supplementary Figure 2](#)). A lower extent of growth retardation was observed for *S. epidermidis* strains, whereas the effect was somewhat more pronounced on the biofilm-forming strain ([Supplementary Figure 2C](#) and [D](#)). As previously detected and presented in [Supplementary Figure 1](#), no effect of COAM was observed on the growth of *P. aeruginosa* ([Supplementary Figure 2E](#)).

Secondly, it is relevant to discriminate whether the antimicrobial effect of COAM is bacteriostatic or bactericidal. The MIC of COAM (2000 µg/mL) and its two- and four-fold higher concentrations were used to determine the MBC (Minimum

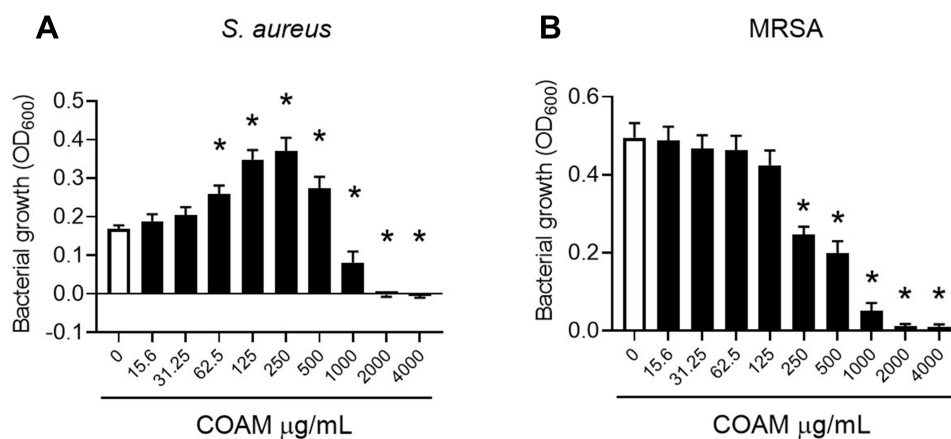


Figure 1 Antimicrobial activity of COAM on *Staphylococcus*. **(A)** *S. aureus* (ATCC 6538P) and **(B)** MRSA (UZ Gasthuisberg collection) growth in Mueller-Hinton broth exposed to increasing concentrations of COAM. 3 independent experiments performed in triplicates (n=3). Data are the mean \pm SEM. *p < 0.05 vs control group without COAM.

Bactericidal Concentration) in the case of *S. aureus* ATCC 6538P and MRSA. After the incubation of pre-grown strains with COAM, we observed that doses of 4000 $\mu\text{g/mL}$ and 8000 $\mu\text{g/mL}$ yielded long-term reductions in the viability of the bacteria, determined using the CFU assay (Figure 2A and B). By comparison of the percentages of bacterial counts in COAM-treated samples with the initial bacterial inoculum, we observed over 99.9% decrease in viability with concentrations 4000 $\mu\text{g/mL}$ and 8000 $\mu\text{g/mL}$ of COAM. Specifically, the incubation of *S. aureus* ATCC 6538P and MRSA with 4000 $\mu\text{g/mL}$ COAM resulted in 0.012% and 0.050% viability, relative to the initial inoculum, respectively. At concentration of 8000 $\mu\text{g/mL}$, the viabilities were 0.005% and 0.077%, respectively. These data suggested a bactericidal activity of COAM on *S. aureus* ATCC 6538P and MRSA, and we determined the MBC of COAM as 4000 $\mu\text{g/mL}$.

Considering the specific antimicrobial effect of COAM in vitro, we wondered whether COAM could act as a therapeutic agent for the treatment of infected wounds. Mouse skin wounds were inoculated with *S. aureus* or MRSA in association or not with COAM. Although COAM had an antimicrobial effect in vitro, we observed that the treatment of infected wounds with COAM at the applied dose was not able to reduce the bacterial colonization of infected wounds, evaluated 2 days after the infection (Figure 2C).

Full Thickness Skin Wounding Alters Leukocyte Contents Extensively

Considering our attempts to modulate various types of migrating host immune cells (eg neutrophils, monocytes/macrophages and lymphocytes) towards better wound healing,⁵ we first optimized the wound healing model of full-thickness skin excision for the study of infiltrating cells. Along with different animal models of wound repair, the full-thickness skin excision model is well known and commonly used.²⁷ Following standardized skin injury, we compared leukocyte subpopulations versus intact skin. To define specific cell types quantitatively and reproducibly, we used flow cytometry analysis of single cell suspensions of the tissues harvested. By analysis of total leukocytes (CD45⁺ cells), neutrophils (CD45⁺, CD11b⁺, Ly6G⁺ cells) and skin macrophages (CD45⁺, CD11b⁺, Ly6G⁻, F4/80⁺ cells) we showed significant alterations in leukocyte populations after wounding (Figure 3 and Supplementary Figure 3). An increase in the total leukocyte population was observed within the first day of injury, which persisted to the third day (Figure 3A). Within this high leukocyte influx, a wave of polymorphonuclear neutrophils infiltrating the wounded skin was evident and this changed the resident population of leukocytes by a neutrophil population consisting of more than 60% of the total leukocytes (Figure 3B-D).

COAM Does Not Alter Maximal Neutrophil Influx Up to 40 Hours After Acute Skin Wounding

With the insight that COAM changes the composition of leukocytes subsets in vivo in dermal air pouches with intact epithelium,¹⁹ we investigated if COAM could also act as a pharmacological modulator in the mouse model of skin

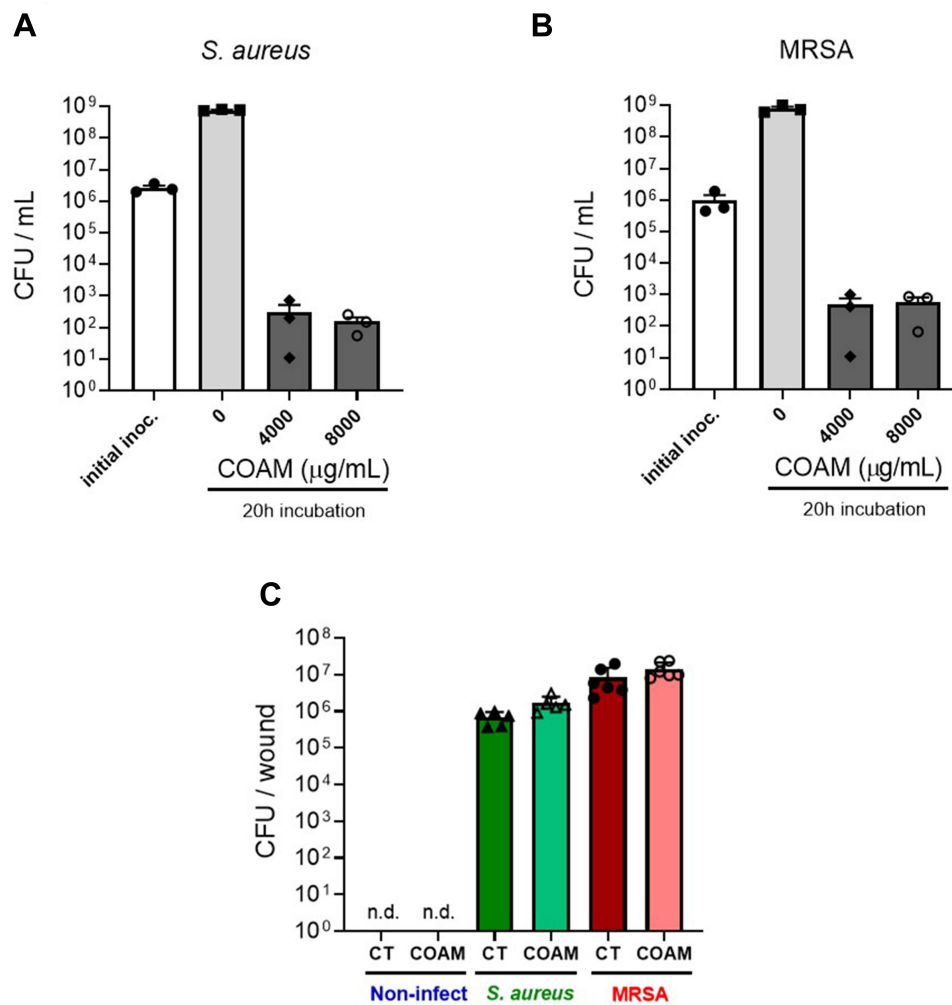


Figure 2 Long-term viability reduction of *Staphylococcus* variants by COAM in vitro. Bacterial viability (CFU/mL) after incubation of (A) *S. aureus* (ATCC 6538P) and (B) MRSA (UZ Gasthuisberg collection) in Mueller-Hinton broth exposed to COAM. 3 independent experiments (n=3). Data are the means \pm SEM. (C) Bacteria colonization determined in skin wounds infected with *S. aureus* (green bars) and MRSA (red bars), 2 days after infection. For each strain, a control group (saline) and COAM group was included. Each data point represents a single mouse (n= 5–6) from which 2 independent wounds were analyzed. n.d., non-detected.

wounds. We confirmed that skin wounding yielded significant changes in skin cell populations towards high frequencies of leukocytes (Figure 4A, vehicle vs intact skin). When COAM was added to the wounds at different doses, no additive effect on neutrophil influx was observed (Figure 4B and C). The recruited neutrophil populations were shown as both frequencies of live cells (Figure 4B) and frequencies within the leukocyte populations in the wounds (Figure 4C). As a comparison, we added the reference values to the known COAM effect in the air pouch model¹⁹ (Panel C, horizontal striped line) and we concluded that COAM has no additive nor inhibitory effect on the maximal neutrophil changes at 24 hours (short-term) post-wounding. To reinforce the previous data, we extended the observation time interval with 16 hours, followed by the application of COAM at different doses and flow cytometry analysis 24 hours later (ie at 40 hours post-wounding). The bottom panels of Figure 4 show that full-thickness skin excision yields maximal neutrophil changes that are not modified by COAM up to 40 hours after wounding.

COAM Alters Monocyte Influx into Sterile Skin Wounds

Neutrophils are first-line defense cells⁵ and bring along pro-angiogenic factors, including VEGF-A and reciprocally a neutrophil subset with pro-angiogenic matrix metalloproteinase-9.^{28–30} This feedback loop, the knowledge that monocyte/macrophage counts were maximal at a later stage in skin wound healing⁵ and the fact that the latter cell type comes with a subset of proangiogenic monocytes³¹ prompted us to study the effect of COAM further. To

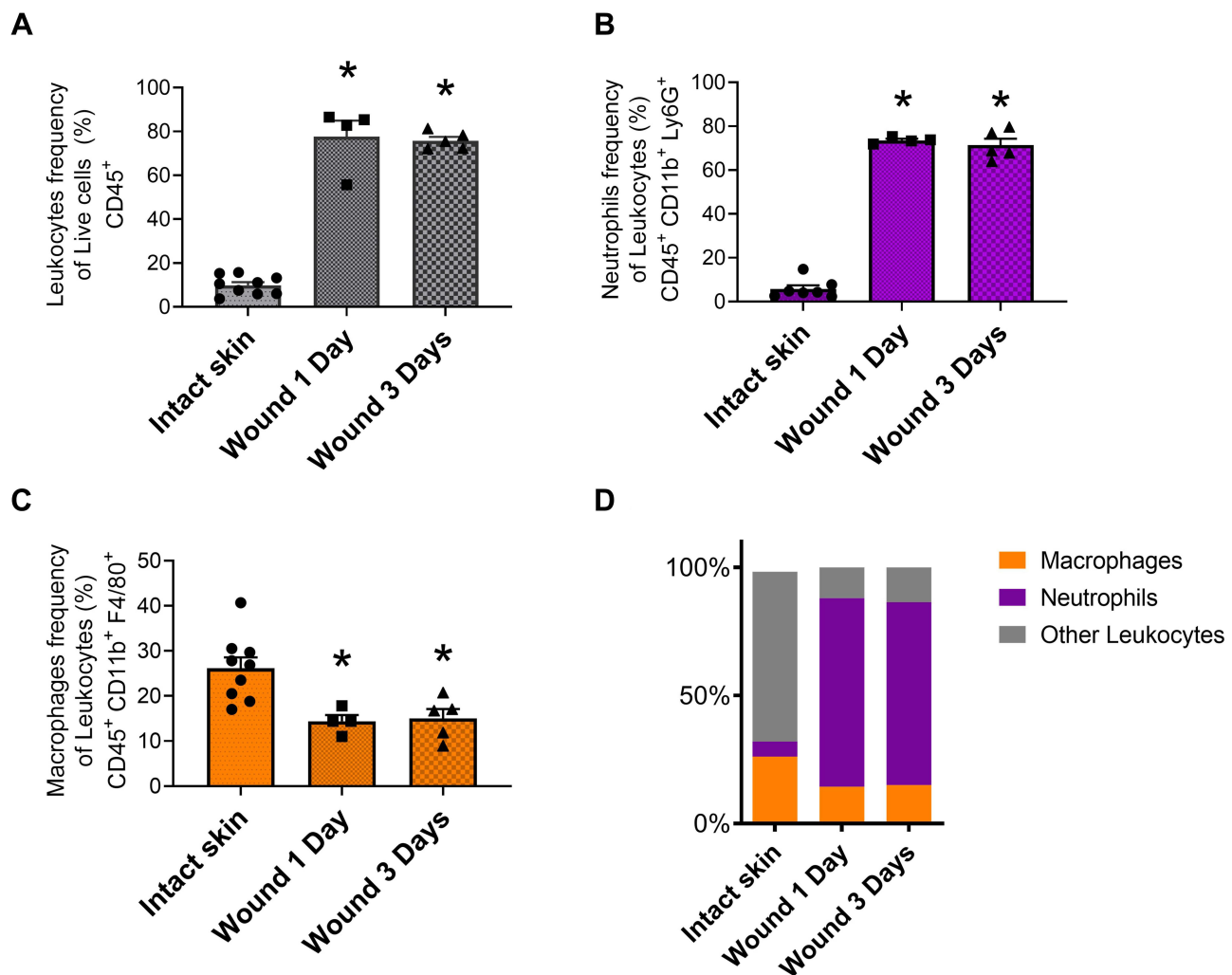


Figure 3 Leukocyte influx into skin wounds. Leukocyte accumulation in skin wounds was analyzed at day 1 and day 3 post-injury and compared with intact skin. **(A)** Leukocytes frequency (CD45⁺) plotted as percentage of live cells. **(B)** Neutrophils (CD45⁺, CD11b⁺ and Ly6G⁺) and **(C)** macrophages (CD45⁺, CD11b⁺, Ly6G⁺, F4/80⁺) frequencies plotted as percentages of leukocytes. **(D)** Relative percentages of leukocytes illustrating population changes (Orange column: macrophages, purple column: neutrophils, gray column: other leukocytes). Data are the mean \pm SEM. * $p < 0.05$ vs intact skin. Each data point represents a single mouse ($n = 4-5$) from which a pool of 2 wounds were analyzed.

complement our descriptive data on monocytes/macrophages, these cells were functionally studied in a mouse model with genetically engineered monocytes/macrophages. Monocyte/macrophage influxes were visualized with the use of an in vivo imaging system in CX₃CR1-GFP mice with and without COAM-treated full thickness skin wounds. CX₃CR1 monocyte/macrophage recruitment, measured as fluorescence intensity, was significantly increased at days 1, 3 and 4 in COAM-treated mice compared to the control mice (Figure 5A). In Figure 5B the higher monocyte/macrophage recruitment to the wound in a COAM-treated mouse was compared to that of a control mouse (1 day after wound). The fluorescence intensity of the wounds in COAM-treated CX₃CR1-GFP mice was more than twice as high as that of vehicle-treated CX₃CR1-GFP mice, whereas the fluorescence intensity from the CX₃CR1-GFP control mice was about 20 times higher than that from the wounds in control mice without the reporter gene construct. The latter comparison demonstrated low background autofluorescence and thus indicated that the signal detected in the IVIS system was from the CX₃CR1-GFP monocytes/macrophages only. Whereas an increased early recruitment of monocytes/macrophages to the wound by treatment with COAM was observed, the associated differences in wound repair were modest. The wound sizes were expressed as wound area on each day and as percent healed wounds in relation to the initial wound size (Figure 6A and B, respectively). We observed a significant reduction in wound sizes at days 1 and 2 (Figure 6A). When

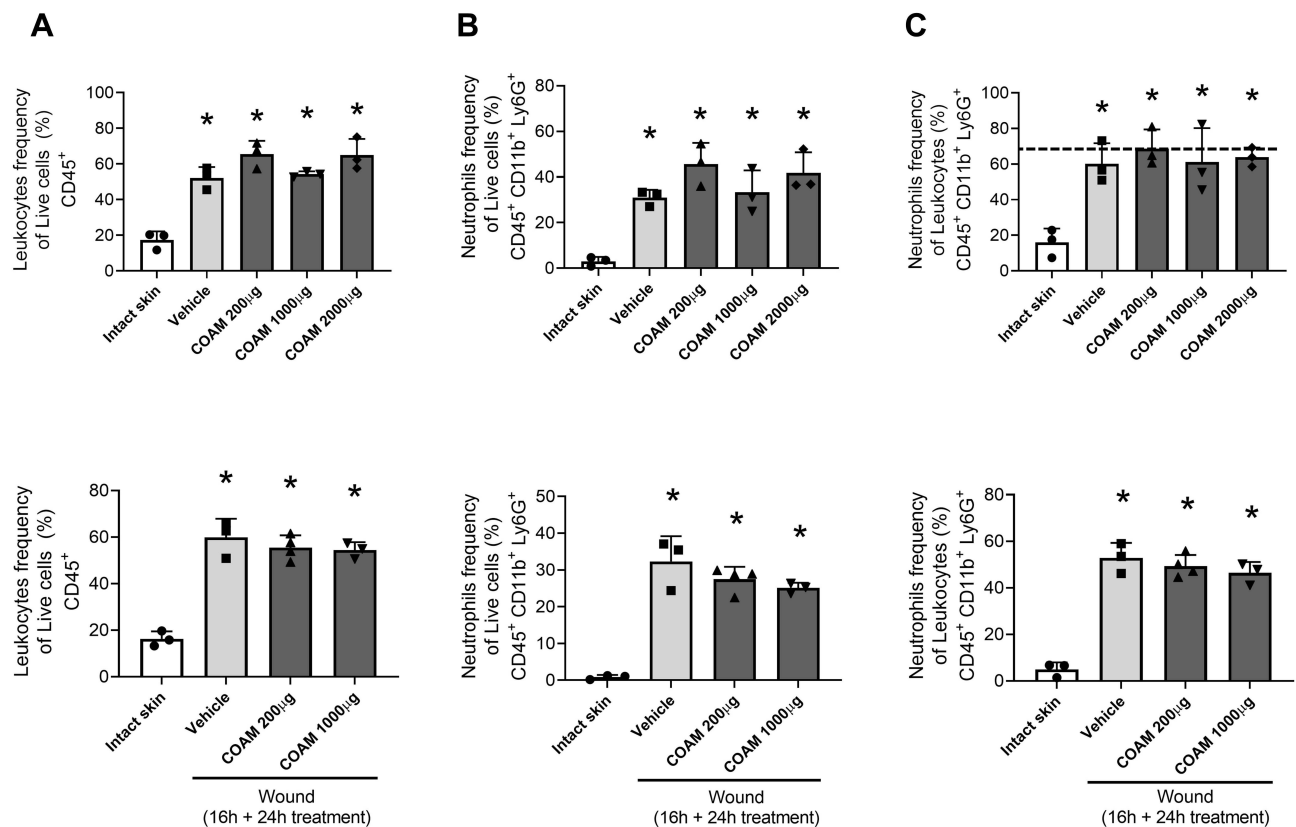


Figure 4 Effect of COAM on neutrophil influx into skin wounds. Neutrophil infiltration in skin wounds was analyzed 24 h after treatment with COAM. COAM treatment was applied into the wounds immediately (upper panel) or 16 h after wounding (bottom panel). (A) Leukocyte (CD45⁺) plotted as percentages of live cells, neutrophils (CD45⁺, CD11b⁺ and Ly6G⁺) plotted as (B) percentages of live cells and as (C) percentages of leukocytes. Data are the mean \pm SEM. * $p < 0.05$ vs intact skin. Each data point represents a single mouse ($n = 3-4$) from which 3 pools of 2 wounds were analyzed.

analyzing the wound healing, an accelerated wound repair on day 2 was observed (Figure 6B). Although no significant differences in sizes or percentages of wound healing were detected at later time points of the healing process, it was evident that the wounds in COAM-treated mice healed faster at an earlier time point (Figure 6C).

Discussion

In this study, we increased the insights on the biological actions of COAM by (i) defining its antibacterial activity against specific skin-related bacterial species and (ii) confirming monocyte influx modulations during the inflammatory stage of full-thickness skin wounds.

A variety of natural polymers have been described to possess significant antimicrobial activity, including polysaccharides such as chitosan, various exopolysaccharides (EPS) and sulphated polysaccharides.¹² Importantly, chemical modifications can alter the structure of polysaccharides and modify their properties, including antimicrobial activity.³² COAM was synthesized already 50 years ago as an antiviral agent intended to mimic the polymeric structure and the molecular charge distribution of viral double-stranded RNA.²⁰ COAM is synthesized by a two-step oxidation process starting from the polysaccharide amylose. The addition of carboxyl groups provides COAM with a polyanionic nature. Our initial experiments indicated that the growth-retarding effect of COAM was the highest against Gram-positive bacteria, especially the *Staphylococcus* species, while it was somewhat lower in the case of *Bacillus* species, whereas it was absent in the case of Gram-negative bacteria such as *Escherichia coli* (Supplementary Figure 1). Considering the fact that staphylococci, including MRSA, frequently cause dermal infections, we performed further experiments on these bacteria. We confirmed the antibacterial effects of COAM against *Staphylococcus aureus* and MRSA, and determined the MIC of COAM as 2000 $\mu\text{g/mL}$. Similar MIC values have also been described for sulphated EPS against *S. aureus*. Interestingly, this chemically modified EPS was shown to possess higher antimicrobial activity than its non-sulphated

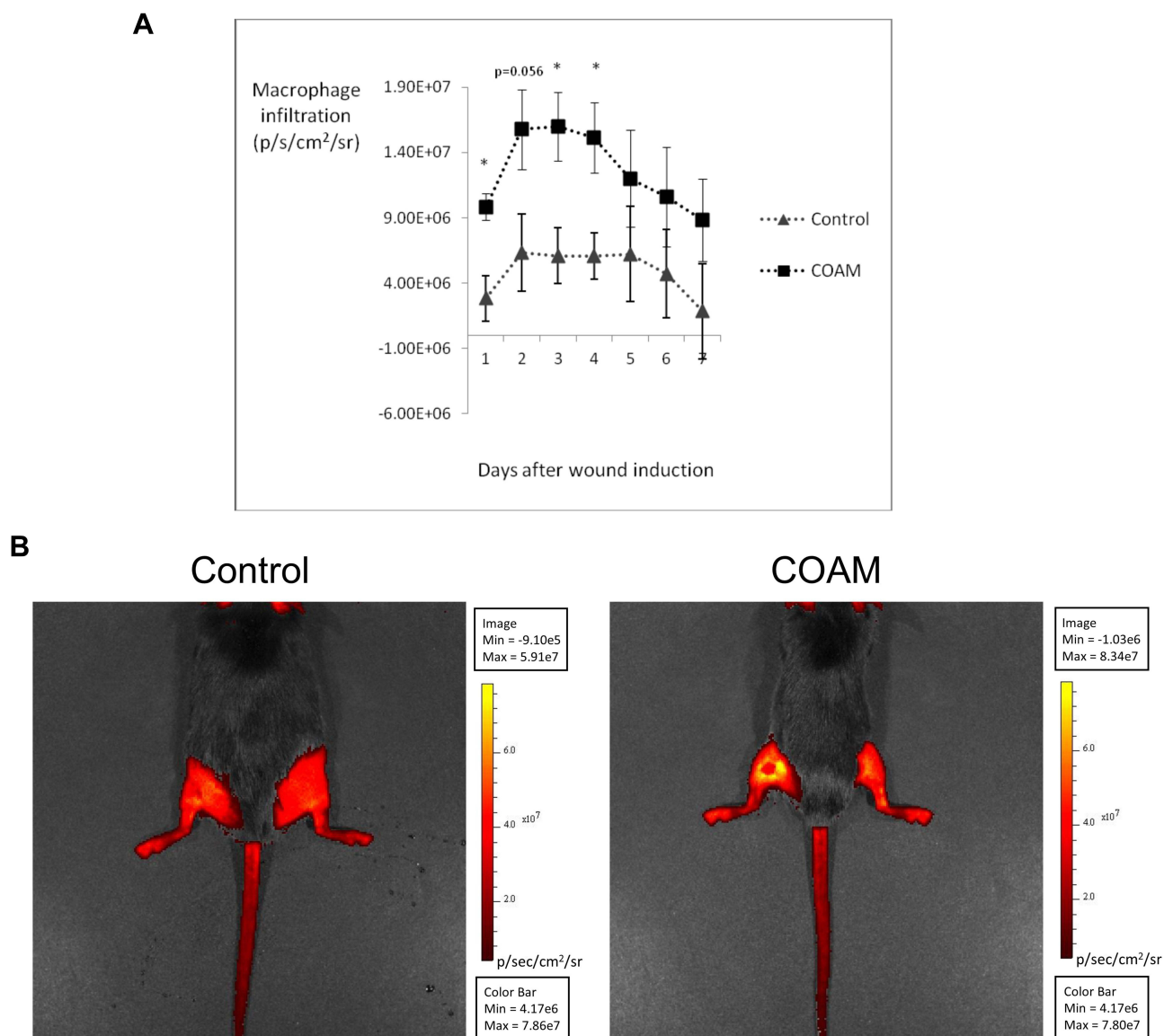


Figure 5 Effect of COAM on monocyte/macrophage infiltration into mouse skin wounds. **(A)** Macrophage infiltration in the wound area of control and COAM-treated CX₃CR1-GFP mice, measured as radiance (p/s/cm²/sr) between day 1 and 7 post-wounding. n=8, *p < 0.05 vs Control group. **(B)** Illustrations of macrophage infiltration 1 day after wound induction in a control and in a COAM-treated mouse. Induced wounds are located on the left hindlimbs for both mice (dorsal photographs). The higher intensity in the wound of COAM-treated mouse corresponds to more macrophage recruitment.

form (MIC values of 2 mg/mL and 6 mg/mL, respectively).³³ Another widely recognized polysaccharide with good antibacterial activities is chitosan. Although chitosan has stronger antimicrobial activity than COAM and EPS, its use is limited to acidic conditions due to poor solubility in neutral environment.³⁴ To overcome this limitation, chemical modifications are also commonly applied to chitosan. These modifications give rise to chitosan derivatives, which possess a very wide range of antimicrobial activity and MIC values.³⁵

Considering that COAM did not inhibit the growth of *Pseudomonas aeruginosa* and *Escherichia coli* (both these species are Gram-negative bacteria), we suppose that it has a quite narrow antibacterial spectrum being active on mostly Gram-positive bacteria such as *Staphylococcus* and *Bacillus*. In the study of Zi et al (2018), it was suggested that the antibacterial effects of similar amylose derivatives are mediated through pH alterations induced by carboxyl groups.³⁶ In our study, no differences in pH were detected between the groups and, therefore, our observed reductions in bacterial growth induced by COAM were not due to pH alterations (data not shown). Our data suggest that other mechanisms may be involved in the antimicrobial effect of COAM. Indeed, the activities of antibacterial polymers, hydrogels and scaffolds

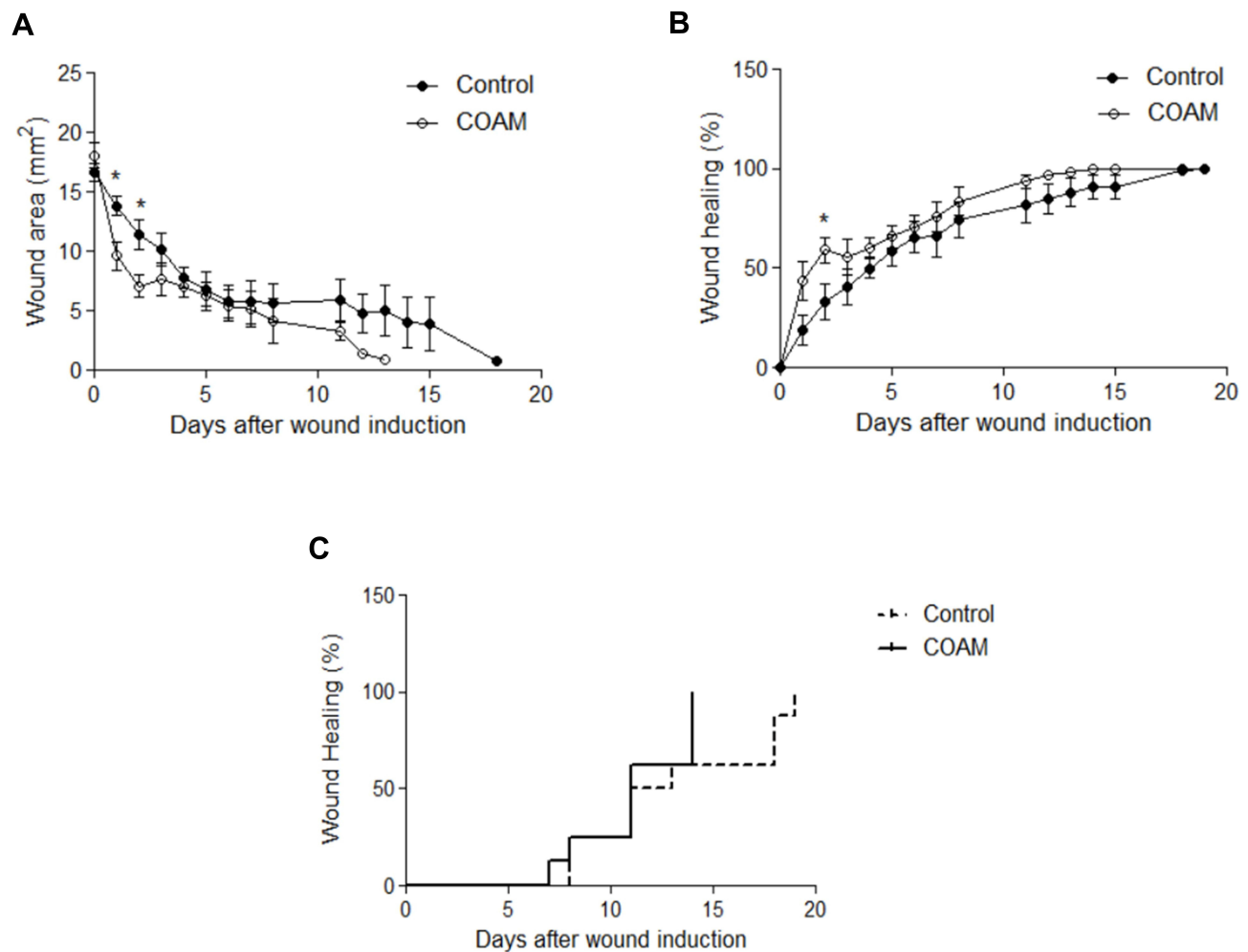


Figure 6 Wound repair in response to COAM treatment. Wound sizes measured until complete closure in control and COAM-treated CX₃CR1-GFP mice. Wound sizes were expressed both as **(A)** wound areas per day and as **(B)** percent healed in relation to the initial wound sizes. **(C)** Kaplan-Meier analysis illustrating at which time point the wounds healed. n=8, *p < 0.05 vs Control group.

provide alternative explanations of action mechanisms, as recently reviewed. These mechanisms include decrease of biofilm formation, disturbance of bacterial membrane integrity, harmful impact on metabolism and other toxic effects.^{12,15,16}

Although in many studies COAM was confirmed to possess a broad antiviral spectrum and a good safety index, it was not further developed as an antiviral agent and its mechanism of action has remained controversial for a long time.³⁷ With recent technologies and better views on immune cells and molecules against viruses, it was shown that COAM potently activates an innate cellular antiviral response.¹⁷ Aside from chemokine induction, COAM also binds to chemokines. Because COAM has higher affinities for specific chemokines than endogenous GAGs, it may locally concentrate bound chemokines. This occurs in such a way that the COAM-bound chemokines retain their chemo-attractive activity.²⁶ In addition, because of its polymeric nature and in contrast to chemokines, COAM has limited tissue diffusion, retaining it at the site of application (eg, injection in wound edges). In this way, COAM-bound chemokines create strong local gradients, and COAM may therefore have additional activities as an immunomodulator in topical applications. With all combined characteristics, COAM creates strong chemotaxis *in vivo* into mouse skin with intact epithelial and dermal layers.¹⁹

In the present study, no changes were observed in neutrophil numbers after supplementation of COAM to the open wounds, in comparison with the vehicle. The wounding itself (control vehicle) yielded maximal influxes of neutrophils, which corresponded to the maximal levels obtainable in the air pouch mouse model with intact skin.¹⁹ Therefore, the use of COAM for induction of local neutrophil influx and the inherent host-protective effects of neutrophils in skin wounds

may be limited to pathological wound healing conditions, eg, in neutropenic patients after chemotherapy or after exposure to therapeutic or accidental radiation.

For macrophages, which are recruited into open skin wounds at later time intervals than neutrophils,⁵ different observations were made. Indeed, COAM amplified the endogenous signals evoked by wound induction, thus significantly recruiting more CX₃CR1 monocytes/macrophages to the wounds compared to what was observed in control mice. In addition, increased macrophage recruitment coincided with an accelerated early wound healing process. Aside from the number of macrophages, their functionality is essential for skin wound repair. The phenotypic switch from a pro-inflammatory phenotype to an anti-inflammatory profile contributes to the resolution of the inflammatory phase and consequently the transition into the proliferative phase.³⁸ Lucas et al (2010) clearly showed through conditionally macrophage-depleted mice that the role of these inflammatory cells differs according to the wound healing phase.³⁹ Although we have not further characterized the phenotype of infiltrated macrophages, the expression of CX₃CR1 regulates multiple reparative processes in skin wound healing and is associated with a more resolute profile in macrophages.^{40,41} For instance, the failure of maturation into CX₃CR1^{hi} macrophages, observed in diabetic wounds, contributes to a persistent inflammatory stage and impairment of the resolution of inflammation.⁴² Therefore, the use of COAM to promote CX₃CR1 monocyte/macrophage recruitment may be an attractive strategy in chronic inflammatory environments. Future experiments will be directed at defining the molecular mechanisms involved in this observation. Additional limitations exist in the present work. First, follow-up studies will be needed to fully demonstrate the clinical effects of COAM on wound healing and whether its antiviral or antibacterial effects are useful. Because open skin wounds already provide maximum neutrophil influx, the effects of COAM may be limited to mononuclear cells, including hematopoietic precursor cells. Hematopoietic precursor cells are claimed to possess regenerative capacities. Alternatively, the neutrophil-potentiating effect of COAM may only become relevant in neutropenic patients, who form only a small subgroup of the cohort of skin wound patients.

Conclusion

Aside from its broad antiviral activity, COAM has an antibacterial effect *in vitro* which was selective against Gram-positive bacteria but not detected for tested Gram-negative bacterial species. The highest antibacterial effect of COAM was detected against skin-associated staphylococci. Furthermore, COAM has immunomodulatory effects *in vivo*, which are here extended to skin wound healing, and these effects deserve further exploration.

Author Contributions

All authors made substantial contributions to conception and design, acquisition of data, or analysis and interpretation of data; took part in drafting the article or revising it critically for important intellectual content; agreed to submit to the current journal; gave final approval for the version to be published; and agreed to be accountable for all aspects of the work.

Funding

The present study was supported by the Rega Foundation, the Fund for Scientific Research of Flanders (FWO – Vlaanderen, G0A5716N) and C1 Funding from KU Leuven. The microbiology studies were partly funded by the Estonian Research Council (grant PUT1050 to TA) and University of Tartu Feasibility Fund (grant PLTMRARENG1 to TV).

Disclosure

Professor Mia Phillipson reports personal fees from Ilya pharma, outside the submitted work;

Dr Triinu Visnapuu reports personal fees from the University of Tartu, outside the submitted work;

Professor Ghislain Opendakker reports grants from the Research Foundation of Flanders (FWO-Vlaanderen), during the conduct of the study. The authors report no other conflicts of interest in this work.

References

1. Ohnstedt E, Lofton Tomenius H, Vågesjö E, Phillipson M. The discovery and development of topical medicines for wound healing. *Expert Opin Drug Discov.* 2019;14(5):485–497.
2. Caporarello N, D'Angeli F, Cambria MT, et al. Pericytes in Microvessels: from “Mural” Function to Brain and Retina Regeneration. *Int J Mol Sci.* 2019;20:24.
3. Wang Y, Tian M, Wang F, et al. Understanding the Immunological Mechanisms of Mesenchymal Stem Cells in Allogeneic Transplantation: from the Aspect of Major Histocompatibility Complex Class I. *Stem Cells Dev.* 2019;28(17):1141–1150.
4. Berhane CC, Brantley K, Williams S, Sutton E, Kappy C. An evaluation of dehydrated human amnion/chorion membrane allografts for pressure ulcer treatment: a case series. *J Wound Care.* 2019;28(Sup5):S4–S10.
5. Opdenakker G, Van Damme J, Vranckx JJ. Immunomodulation as Rescue for Chronic Atonic Skin Wounds. *Trends Immunol.* 2018;39(4):341–354.
6. Rahim K, Saleha S, Zhu X, Huo L, Basit A, Franco OL. Bacterial Contribution in Chronicity of Wounds. *Microb Ecol.* 2017;73(3):710–721.
7. Percival SL, Emanuel C, Cutting KF, Williams DW. Microbiology of the skin and the role of biofilms in infection. *Int Wound J.* 2012;9(1):14–32.
8. Filius PM, Gyssens IC. Impact of increasing antimicrobial resistance on wound management. *Am J Clin Dermatol.* 2002;3(1):1–7.
9. Choodari Gharehpapagh A, Farahpour MR, Jafarirad S. The biological synthesis of gold/perlite nanocomposite using *Urtica dioica* extract and its chitosan-capped derivative for healing wounds infected with methicillin-resistant *Staphylococcus aureus*. *Int J Biol Macromol.* 2021;183:447–456.
10. Daghighan SG, Farahpour MR, Jafarirad S. Biological fabrication and electrostatic attractions of new layered silver/talc nanocomposite using *Lawsonia inermis* L. and its chitosan-capped inorganic/organic hybrid: investigation on acceleration of *Staphylococcus aureus* and *Pseudomonas aeruginosa* infected wound healing. *Mater Sci Eng C Mater Biol Appl.* 2021;128:112294.
11. Pourkarim R, Farahpour MR, Rezaei SA. Comparison effects of platelet-rich plasma on healing of infected and non-infected excision wounds by the modulation of the expression of inflammatory mediators: experimental research. *Eur J Trauma Emerg Surg.* 2022. ;48(4):3339–3347.
12. Wang ZC, Sun Q, Zhang HR, et al. Insight into antibacterial mechanism of polysaccharides: a review. *Lwt-Food Sci Technol.* 2021;2:150.
13. Abdalla AK, Ayyash MM, Olaimat AN, et al. Exopolysaccharides as Antimicrobial Agents: mechanism and Spectrum of Activity. *Front Microbiol.* 2021;12:664395.
14. Jeong D, Kim DH, Kang IB, et al. Characterization and antibacterial activity of a novel exopolysaccharide produced by *Lactobacillus kefirano-faciens* DNI isolated from kefir. *Food Control.* 2017;78:436–442.
15. Alavi M, Nokhodchi A. An overview on antimicrobial and wound healing properties of ZnO nanobiofilms, hydrogels, and bionanocomposites based on cellulose, chitosan, and alginate polymers. *Carbohydr Polym.* 2020;227:115349.
16. Pamu D, Tallapaneni V, Karri V, Singh SK. Biomedical applications of electrospun nanofibers in the management of diabetic wounds. *Drug Deliv Transl Res.* 2022;12(1):158–166.
17. Li S, Starckx S, Martens E, et al. Myeloid cells are tunable by a polyanionic polysaccharide derivative and co-determine host rescue from lethal virus infection. *J Leukoc Biol.* 2010;88(5):1017–1029.
18. Berghmans N, Heremans H, Li S, et al. Rescue from acute neuroinflammation by pharmacological chemokine-mediated deviation of leukocytes. *J Neuroinflammation.* 2012;9:243.
19. Vandooren J, Berghmans N, Dillen C, et al. Intradermal air pouch leukocytosis as an in vivo test for nanoparticles. *Int J Nanomedicine.* 2013;8:4745–4756.
20. Claes P, Billiau A, De Clercq E, et al. Polyacetal carboxylic acids: a new group of antiviral polyanions. *J Virol.* 1970;5(3):313–320.
21. Li S, Martens E, Dillen C, Van den Steen PE, Opdenakker G. Virus entry inhibition by chlorite-oxidized oxyamylose versus induction of antiviral interferon by poly(I:C). *Biochem Pharmacol.* 2008;76(7):831–840.
22. Brubaker AL, Carter SR, Kovacs EJ. Experimental Approaches to Tissue Injury and Repair in Advanced Age. *Methods Mol Biol.* 2015;1343:35–51.
23. Hoffmann JP, Friedman JK, Wang Y, et al. In situ Treatment With Novel Microbiocide Inhibits Methicillin Resistant *Staphylococcus aureus* in a Murine Wound Infection Model. *Front Microbiol.* 2019;10:3106.
24. Vågesjö E, Ohnstedt E, Mortier A, et al. Accelerated wound healing in mice by on-site production and delivery of CXCL12 by transformed lactic acid bacteria. *Proc Natl Acad Sci U S A.* 2018;115(8):1895–1900.
25. Li Z, Gothard E, Coles MC, Ambler CA. Quantitative Methods for Measuring Repair Rates and Innate-Immune Cell Responses in Wounded Mouse Skin. *Front Immunol.* 2018;9:347.
26. Li S, Pettersson US, Hoorelbeke B, et al. Interference with glycosaminoglycan-chemokine interactions with a probe to alter leukocyte recruitment and inflammation in vivo. *PLoS One.* 2014;9(8):e104107.
27. Wong VW, Sorkin M, Glotzbach JP, Longaker MT, Gurtner GC. Surgical approaches to create murine models of human wound healing. *J Biomed Biotechnol.* 2011;2011:969618.
28. Loffredo S, Borriello F, Iannone R, et al. Group V Secreted Phospholipase A2 Induces the Release of Proangiogenic and Antiangiogenic Factors by Human Neutrophils. *Front Immunol.* 2017;8:443.
29. Christoffersson G, Vagesjo E, Vandooren J, et al. VEGF-A recruits a proangiogenic MMP-9-delivering neutrophil subset that induces angiogenesis in transplanted hypoxic tissue. *Blood.* 2012;120(23):4653–4662.
30. Bekes EM, Schweighofer B, Kupriyanova TA, et al. Tumor-recruited neutrophils and neutrophil TIMP-free MMP-9 regulate coordinately the levels of tumor angiogenesis and efficiency of malignant cell intravasation. *Am J Pathol.* 2011;179(3):1455–1470.
31. Zajac E, Schweighofer B, Kupriyanova TA, et al. Angiogenic capacity of M1- and M2-polarized macrophages is determined by the levels of TIMP-1 complexed with their secreted proMMP-9. *Blood.* 2013;122(25):4054–4067.
32. Cumpstey I. Chemical modification of polysaccharides. *ISRN Org Chem.* 2013;2013:417672.
33. Zhang J, Cao Y, Wang J, et al. Physicochemical characteristics and bioactivities of the exopolysaccharide and its sulphated polymer from *Streptococcus thermophilus* GST-6. *Carbohydr Polym.* 2016;146:368–375.
34. Rabea EI, Badawy ME, Stevens CV, Smaghe G, Steurbaut W. Chitosan as antimicrobial agent: applications and mode of action. *Biomacromolecules.* 2003;4(6):1457–1465.
35. Sahariah P, Masson M. Antimicrobial Chitosan and Chitosan Derivatives: a Review of the Structure-Activity Relationship. *Biomacromolecules.* 2017;18(11):3846–3868.

36. Zi Y, Zhu M, Li X, et al. Effects of carboxyl and aldehyde groups on the antibacterial activity of oxidized amylose. *Carbohydr Polym.* 2018;192:118–125.
37. Opendakker G, Li S, Berghmans N, Damme JV. Applications of glycobiology: biological and immunological effects of a chemically modified amylose-derivative. In: *Carbohydrate Chemistry*. Vol. 38. The Royal Society of Chemistry; 2012:1–12.
38. Boniakowski AE, Kimball AS, Jacobs BN, Kunkel SL, Gallagher KA. Macrophage-Mediated Inflammation in Normal and Diabetic Wound Healing. *J Immunol.* 2017;199(1):17–24.
39. Lucas T, Waisman A, Ranjan R, et al. Differential roles of macrophages in diverse phases of skin repair. *J Immunol.* 2010;184(7):3964–3977.
40. Varga T, Mounier R, Horvath A, et al. Highly Dynamic Transcriptional Signature of Distinct Macrophage Subsets during Sterile Inflammation, Resolution, and Tissue Repair. *J Immunol.* 2016;196(11):4771–4782.
41. Ishida Y, Gao JL, Murphy PM. Chemokine receptor CX3CR1 mediates skin wound healing by promoting macrophage and fibroblast accumulation and function. *J Immunol.* 2008;180(1):569–579.
42. Burgess M, Wicks K, Gardasevic M, Mace KA. Cx3CR1 Expression Identifies Distinct Macrophage Populations That Contribute Differentially to Inflammation and Repair. *Immunohorizons.* 2019;3(7):262–273.

Journal of Inflammation Research

Dovepress

Publish your work in this journal

The Journal of Inflammation Research is an international, peer-reviewed open-access journal that welcomes laboratory and clinical findings on the molecular basis, cell biology and pharmacology of inflammation including original research, reviews, symposium reports, hypothesis formation and commentaries on: acute/chronic inflammation; mediators of inflammation; cellular processes; molecular mechanisms; pharmacology and novel anti-inflammatory drugs; clinical conditions involving inflammation. The manuscript management system is completely online and includes a very quick and fair peer-review system. Visit <http://www.dovepress.com/testimonials.php> to read real quotes from published authors.

Submit your manuscript here: <https://www.dovepress.com/journal-of-inflammation-research-journal>